



# Shape Effects on Bearing Capacity of Footings on Two-Layered Clay

Konstantina Papadopoulou · George Gazetas

Received: 27 April 2018 / Accepted: 15 October 2019 / Published online: 26 October 2019  
© Springer Nature Switzerland AG 2019

**Abstract** The undrained vertical bearing capacity on a two-layered clay of centrally loaded rigid strip, rectangular and ring footings is studied parametrically with 2D, 3D and axisymmetric finite-element analyses. The shear strength ratio of the two layers and the relative thickness of the uppermost layer with respect to pertinent foundation dimension are the key parameters investigated. In addition, for rectangles and rings the length-to-width (“aspect”) ratio and the ring width to external radius ratio are reported. The results are portrayed in diagrams of bearing capacity and shape modification factors, in the familiar soil mechanics form, along with fitted algebraic expressions to facilitate their numerical use. The failure mechanisms are presented for a number of characteristic cases and are being contrasted with the classical Prandtl failure mechanism, giving additional insight into the mechanics of the problem. The results of the paper can be directly used in practical applications.

**Keywords** Clays · Bearing capacity · Foundation shape · Failure mechanism · Rectangular footing · Ring footing

## List of Symbols

A Contact area of the footing

B	Width of rectangular footing
b	Width of ring foundation
E	Modulus of elasticity
$H_1$	Thickness of top clay layer
L	Length of rectangular footing
$N_C, N_C^*$	Bearing capacity (B.C.) factors for strip or other footing’s shape, resting on homogeneous soil
$N_{C,1}, N_{C,1}^*$	B.C. factors for strip or other footing’s shape, resting on two-layered clay
$q_o$	Initial step loading on foundation
$q_u$	Ultimate bearing pressure
$R_{int}$	Strength reduction factor of interfaces
$R_1, R_2$	Radii of ring foundation (external and internal)
$s_c$	Shape factor
SR	Strength ratio ( $s_{u,2}/s_{u,1}$ )
$s_u$	Undrained shear strength of homogeneous clay
$s_{u,1}, s_{u,2}$	Undrained shear strength of the crust and the lower clay layer
$V_u$	Ultimate vertical load
$\gamma$	Unit weight
$\lambda_H, \lambda_B$	Correction factors for the contribution of upper and lower clay to the B.C.
$\lambda_N, \lambda_N^*$	Modification coefficients ( $N_{C,1}/N_C, N_{C,1}^*/N_C^*$ )
$\nu$	Poisson’s ratio

K. Papadopoulou (✉) · G. Gazetas  
National Technical University of Athens, Athens, Greece  
e-mail: konstantina\_p1986@yahoo.gr

## 1 Introduction

The bearing capacity (B.C.) of a strip foundation resting on the surface of homogeneous soil under undrained conditions is obtained by Prandtl's classical 2D solution. For the ultimate resistance of square, rectangular and circular footings on homogeneous soil, correction factors are applied to Prandtl's bearing capacity expression (i.e. Hansen, 1970, Vesic, 1975). A detailed review on the subject has been presented by Poulos et al. (2001). Salgado et al. (2004) presented results of rigorous analyses giving definitive values of shape and depth factors for strip, rectangular and circular footings in homogeneous undrained clay, while Nguyen and Merifield (2012) investigated with finite-elements the shape and depth effects on the undrained bearing capacity in homogeneous soil.

Two-layered soils abound in nature. Bearing capacity of a footing will be affected by the properties of both layers if its dimension is relatively large compared to the thickness of the upper layer. This was also extensively investigated with methods ranging from simplified to rigorous. An early approximate modification of the theoretical B.C. formula for a strip in two-layered clay was presented by Button (1953), who used successfully circular slip surfaces (Puzrin et al. 2010). Empirical modifications were presented by Brown and Meyerhof (1969), who utilised model tests results with circular and strip footings, in which punching failure through the top layer developed. Similar proposals were presented by Meyerhof and Hanna (1978). Numerical solutions for both lower and upper bounds were presented by Chen (1975), Michalowski and Shi (1995), Merifield et al. (1999) and Michalowski (2002) for the undrained bearing capacity for strip footings on a two-layered clay. 2D finite element analyses for strip footings on two-layered soil were presented by Burd and Frydman (1997), Zhu (2004) and Benmebarek et al. (2012).

3D F.E. analyses for rectangular foundations over two-layered clays, were presented by Zhu and Michalowski (2005), Merifield and Nguyen (2006). Salgado et al. (2013) re-examined failure cases of foundations in layered soils by 3D F.E. limit analyses, showing off the practical importance of such problems. According to Salgado (2008), the variation of shear strength with depth affects both the depth and shape of the slip mechanism, so a suitable analysis method is necessary. Moayed et al. (2012)

investigated the bearing capacity of ring foundations on two-layered soil (clay and sand), while Lee et al. (2016) presented results for ring foundation on clay layer with linearly increasing undrained shear strength with depth.

In the present paper, a more comprehensive study is reported for rough, rigid footings of various shapes (strip, square, rectangular and ring) on two-layered clays. 2D or 3D F.E. analyses are performed and emphasis is given to evaluation of the results in conjunction with the failure mechanisms. We investigate parametrically two cases depending on the  $SR = s_{u2}/s_{u1}$  ratio:  $SR < 1$  and  $SR > 1$ , which are separately analyzed. The visual understanding of the unfavourable or favourable effects of second layer is facilitated by modification coefficients of the conventional bearing capacity factors.

## 2 Problem Definition and F.E. Simulation

For a strip footing on the surface of homogeneous clay, the ultimate bearing pressure can be written in the form:

$$q_u = \frac{V_u}{B} = N_C s_u \quad (1)$$

where  $V_u$  is the ultimate central load,  $B$  the width of the strip,  $s_u$  the undrained shear strength and  $N_C = 2 + \pi$ , according to Prandtl.

For the case of two-layered undrained clay it is convenient to rewrite Eq. (1), as:

$$q_u = N_{C,1} s_{u,1} \quad (2)$$

where  $s_{u,1}$  the undrained shear strength of the upper clay layer and  $N_{C,1}$  the bearing capacity factor, which depends on the geometry ( $H_1/B$ ) and the strength ratio  $SR = s_{u,2}/s_{u,1}$  (Fig. 1a).

For footings with different shape (rectangular, square, ring), in case of homogeneous clay, Eq. (1) is modified, as:

$$q_u = \frac{V_u}{A} = N_C^* s_u \quad (3)$$

where  $A$  the contact area of the footing and  $N_C^*$  the bearing capacity factor, which encompasses the shape effect (shape factor). Accordingly, for two-layered clay, Eq. (2) can be rewritten in the form:

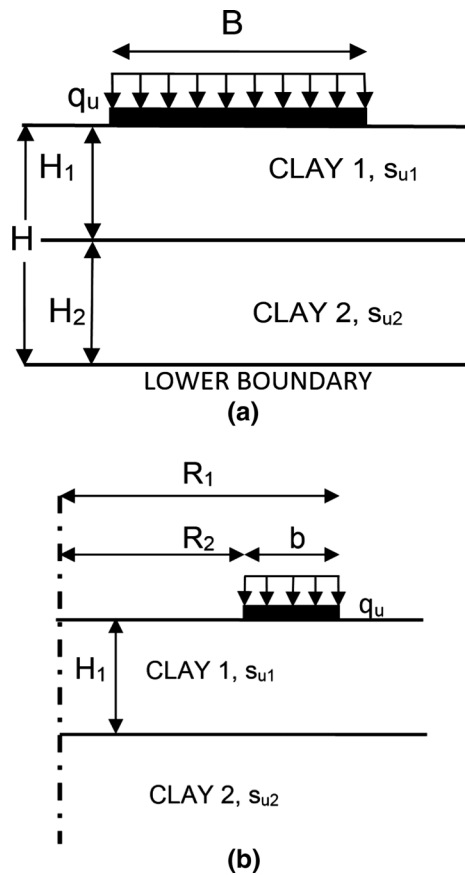


**Fig. 1** Geometrical model of rigid foundation on two-layered clays: **a** strip or rectangular, **b** ring footing

$$q_u = N_{C,1}^* s_{u,1} \tag{4}$$

Now, the modified B.C. factor  $N_{C,1}^*$  is a function of  $H_1/B$ , SR and the aspect ratio  $L/B$  for a rectangular footing or by the ratios  $H_1/R$ , SR and  $b/R_1$  for ring foundation, according to Fig. 1b.

The analyses are carried out with the finite element programs Plaxis. The standard boundary conditions for 2D or axisymmetry are applied, where the F.E. program generates in the  $(x, y)$  plane ( $y$ : vertical direction) full fixity at the base of geometry ( $u_x = u_y = 0$ ) and roller conditions at the vertical sides ( $u_x = 0, u_y = \text{free}$ ). In the 3D model used, the front and end planes are always fixed in the  $z$ -direction ( $u_z = 0$ ). For the soil modeling in 2D conditions 15-node triangular elements are selected, while in 3D, 15-node wedge elements are used by default. In both cases 12 stress points correspond to each element. The contact surface between foundation and soil is modeled with interface

elements, including five pairs of nodes (since the F.E. mesh consists of 15-node elements). The interface elements permit both separation and slip. However, the Mohr–Coulomb criterion is used to distinguish elastic behaviour (where small displacements can occur) and plastic behaviour (where permanent slip may occur), depending on the shear stresses and interface shear strength. Nevertheless, in the present case neither separation nor slip is expected. The overall mesh dimensions in vertical plan view are selected large enough to avoid spurious boundary effects. The thickness of the second layer,  $H_2$ , is large enough to have any effect; hence, for stiff over soft clay ( $SR < 1$ ) the lower boundary is set to depth up to  $6B$  in most cases. On the contrary, for  $SR > 1$  (soft over stiff clay) this depth is selected much smaller, since the failure mechanism is quite shallow. The appropriate refinement of the mesh is provided in the areas of high stress or strain gradient near the vicinity of the footing. A typical 3D mesh is illustrated in Fig. 2 for square footing (case  $H_1/B = 0.5$  and  $H/B = 3$ ), where the area of the mesh refinement is visible. The soil is modeled as linearly elastic-perfectly plastic material obeying Tresca’s failure law. The geotechnical parameters of clay layers used in the analyses are presented in the Table 1. The strength ratio varied between the values  $SR = 0.133 - 5$ , Young’s modulus  $E = 300 s_u$  and Poisson’s ratio  $\nu = 0.495$ . Nevertheless, neither the ratio  $\nu$  nor the modulus  $E$  had any appreciable effect on the resulting ultimate bearing capacity and consequently on the B.C. factors  $N_{C,1}$  or  $N_{C,1}^*$ . The water table was set at the surface. The submerged unit weight of the second layer,  $\gamma_2$  had no effect on the B.C. factors. Nevertheless, the bearing capacity was slightly influenced by the overburden pressure at the interface of the clay layers, as we found out in several preliminary sensitivity analyses with varying  $\gamma_1$  values ( $0 \leq \gamma_1 \leq 20 \text{ kN/m}^3$ ). Indeed, the assumption that the soil can be considered as weightless is accurate only for homogeneous clay under undrained conditions. In this way, Yu et al. (2011) had concluded that in some cases of two-layered clays, the unit weight of the top layer plays a role in the development of the failure mechanism.

In order to calculate the equivalent B.C. factors  $N_{C,1}$  or  $N_{C,1}^*$ , the ultimate pressure, according to Eqs. (2) and (4) is resulted by the incremental

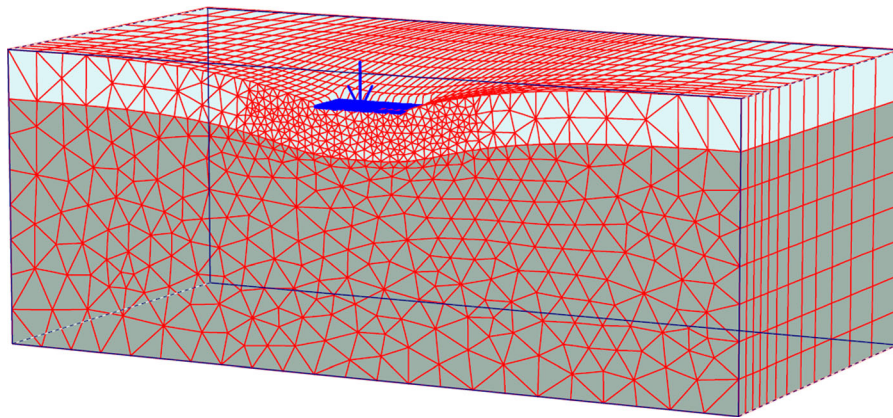


**Fig. 2** Example of F.E. mesh for square footing ( $H_f/B = 0.50$ )

**Table 1** Geotechnical parameters of the two clay layers

Description	Unit weight	Strength parameters		Elastic parameters	
	$\gamma$ (kN/m <sup>3</sup> )	$s_u$ (kPa)	<sup>a</sup> R <sub>int</sub>	E (MPa)	$\nu$
Upper clay layer	20	100	1	30	0.495 (0.3)
Lower clay layer					
(a) $SR \leq 1$	18	13.3–100	1	4–30	0.495 (0.3)
(b) $SR \geq 1$	22	100–500	1	30–150	0.495 (0.3)

<sup>a</sup>R<sub>int</sub>: Strength reduction factor of interfaces

multipliers procedure: Firstly, the foundation is calculated with initial loading  $q_o$  and the gradual increase of the external loading is achieved in only one, next phase, up to failure. From the ultimate loading  $q_u = (N_{C,1}$  or  $N_{C,1}^*) s_{u1}$ , the corresponding B.C. factors are calculated. At the end of this phase, where the increasing factor reaches the maximum value (corresponding to  $q_u$ ), the failure mechanism can be observed through the vectors of total displacements in shadings.

### 3 Shape Factors on a Homogeneous Clay (SR= 1): Comparisons and Verification

The effect of foundation shape is usually expressed through a shape factor  $s_c = N_C^*/N_C$ , where  $N_C$  the B.C. factor for strip and  $N_C^*$  for a non-strip footing for homogeneous soil. The theoretical Prandtl’s factor is  $N_C = 2 + \pi$ , while our finite element analysis gave a slightly higher  $N_C \approx 5.164$ . For rectangular footings on undrained clay ( $\varphi = 0$ ), the available in the literature  $s_c$  relations include:

$$\text{Hansen (1970) : } s_c = 1 + 0.2 \frac{B}{L} \tag{5a}$$

$$\text{Vesic (1975) : } s_c = 1 + 0.194 \frac{B}{L} \tag{5b}$$

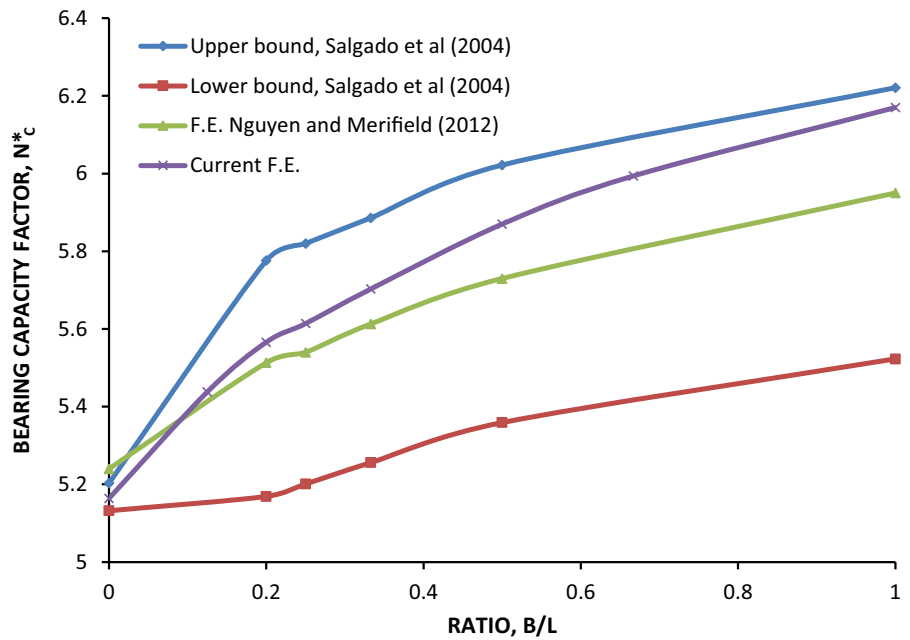
$$\text{Salgado et al. (2004) : } s_c = 1 + C_1 \frac{B}{L} \tag{5c}$$

where the regression constant (for all cases) is:  $0.125 \leq C_1 \leq 0.190$  for  $1 \geq B/L \geq 0.2$

The values  $N_C^*$  from our 3D F.E. analyses for rectangular footings are compared with those from Salgado et al. (2004) and Nguyen and Merifield (2012) in Fig. 3. It is clear that our F.E. results plot in-between the upper and lower bounds of Salgado et al. (2004), while from the comparison with the results after Nguyen and Merifield (2012), the following can be observed:

1. In a wide range of  $B/L$ , our results are higher. Especially for  $1/3 \leq B/L \leq 1$ , the deviation ranges between 1.5 and 3.7%.
2. On the contrary, for lower values of the aspect ratio, our results are lower. In the case of strip footing, Nguyen and Merifield (2012) reported

**Fig. 3** Comparison of results  $N_C^*$  for rectangular footings on homogeneous clay



$N_C = 5.24$ , while our analyses resulted in  $N_C = 5.164$ .

From the current F.E. analyses, the shape factor can be approximated by the following closely-fitted formula:

$$s_c \approx 1 + 0.2(B/L)^{0.60} \tag{6}$$

The deviations of the shape factor according to Eq. (6) from current F.E. results are negligible. However, the deviations from other well-known formulae must be defined:

1. The maximum deviation from the linear relationship (5a) is of the order of 3.3%.
2. In general, our results indicate shape factors higher than those, according to Nguyen and Merifield (2012). The deviations varied between 2.2 and 5.0%, the higher value corresponding to square.
3. Nevertheless, it may be noted that for square footings, our F.E. results gave  $s_c = 1.195$  and Eq. (6)  $s_c = 1.2$ , i.e. values almost identical with other well-established formulae.

For ring footings, Fig. 4 presents the F.E. results, where  $N_C^*$  increases with increasing the “width” ratio  $b/R_1$ , but surprisingly it reaches a peak not at the full circle but at  $b/R_1 \approx 0.9$ , that is for a circle with a

small hole in the center. Evidently, the ultimate bearing pressure depends on the failure mechanism, which is strongly affected by the ratio  $b/R_1$ . Apart from the main failure surface below the width  $b_1$ , a secondary one develops at the region of the ring’s hole. But for very large width (i.e. small hole)  $0.9 \leq b/R_1 \leq 1$ , the total ultimate vertical load,  $V_u = q_u \pi R_1^2 [1 - (1 - b/R_1)^2]$  remains unchanged and thus for increasing the ratio  $b/R_1$  slightly decreases the ultimate pressure  $q_u$  along with the B.C. factor  $N_C^*$ . However, the small difference between the  $N_C^*$  factors for  $b/R_1 = 0.90$  and 1 is only 1%, equal to the difference between the corresponding contact areas. For the shape correction factor, the approximate closed formula from regression analysis is derived from:

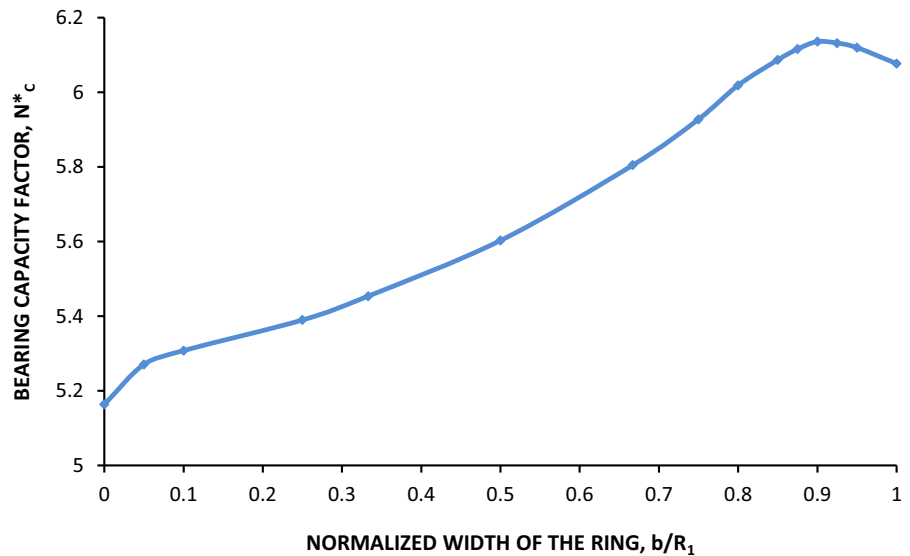
$$s_c \approx 1 + 0.211(b/R_1)^{1.25}, \quad \text{for } 0 < b/R_1 \leq 0.90 \tag{7a}$$

and

$$s_c \approx 1.184, \quad \text{for } 0.9 \leq b/R_1 \leq 1 \tag{7b}$$

The shape factor for the circular footing ( $b/R_1 = 1$ ) according to Eq. (7b), is slightly lower than for the square (Fig. 3). In contrast, Nguyen and Merifield (2012) reported slightly higher  $s_c$  value for circular

**Fig. 4** B.C. factor  $N_C^*$  as a function of the normalized width of ring foundation on homogeneous clay



footing and correspondingly higher values for bearing capacity factor,  $N_C^*$ .

## 4 Stiff Over Soft Clay Layer

### 4.1 Strip Footing

This profile is of interest in geotechnical practice, where soft or medium clay underlays a stiff clayey “crust”. From extended parametric analyses, when  $SR = s_{u,2}/s_{u,1} < 1$ , three failure mechanisms have been observed:

1. A failure mechanism approaching Prandtl’s for relatively high values of SR (approaching homogeneous soil) and/or high values of normalized thickness (type I).
2. Intermediate type (II): The failure planes of the wedge, according to Prandtl, become gradually curved, approaching the vertical direction. This mechanism can be characterized as partial punching, taking place for various combinations of the normalized values  $H_1/B$  and SR.
3. A punching failure, according to Meyerhof and Hanna (1978), which is observed for relatively low values of  $H_1/B$  and/or low SR values (type III).

Quantitative information regarding the bound values of  $H_1/B$  and SR for each mechanism is given in

Fig. 7. Figure 5 illustrates these three mechanisms for strip footings in two-clay layers with  $H_1/B = 0.75$ . Case (a) refers to a high strength contrast,  $SR = 0.133$ , where a punching failure (type III) is clearly developed, despite the rather substantial crust thickness. The failure surface extends to a depth of about  $2.5 B$ , much higher than the theoretical depth of influence for homogeneous clay ( $\approx 0.7 B$ ). Reducing the strength contrast, i.e. increasing SR, leads to modification of the failure mechanism: in case of  $SR = 0.40$  (b), the mechanism is of type II and in case of  $SR = 0.80$  (c), it is essentially type I. From the analyses, an almost linear relationship between  $N_{C,1}$  and  $H_1/B$  is noted for a wide range of SR values. To better visualize this linear relation and the effect of the lower weaker layer on the bearing capacity, we plot the ratio  $\lambda_N = N_{C,1}/N_C$  as a function of the normalized thickness in Fig. 6. For the linear part of diagrams of Fig. 6, we can express the ultimate pressure and the B.C. factor, as:

$$q_u = 2s_{u,1} \frac{H_1}{B} \lambda_H + N_C s_{u,2} \lambda_B = N_{C,1} s_{u,1} \quad (8a)$$

and

$$N_{C,1} = 2 \frac{H_1}{B} \lambda_H + N_C(SR) \lambda_B \quad (8b)$$

where  $N_C = 2 + \pi$  for homogeneous clay and  $\lambda_H, \lambda_B$  are (approximately) functions of SR only, independent of the normalized thickness. It is evident that Eq. (8a) reflects the contribution of shear strength of the two



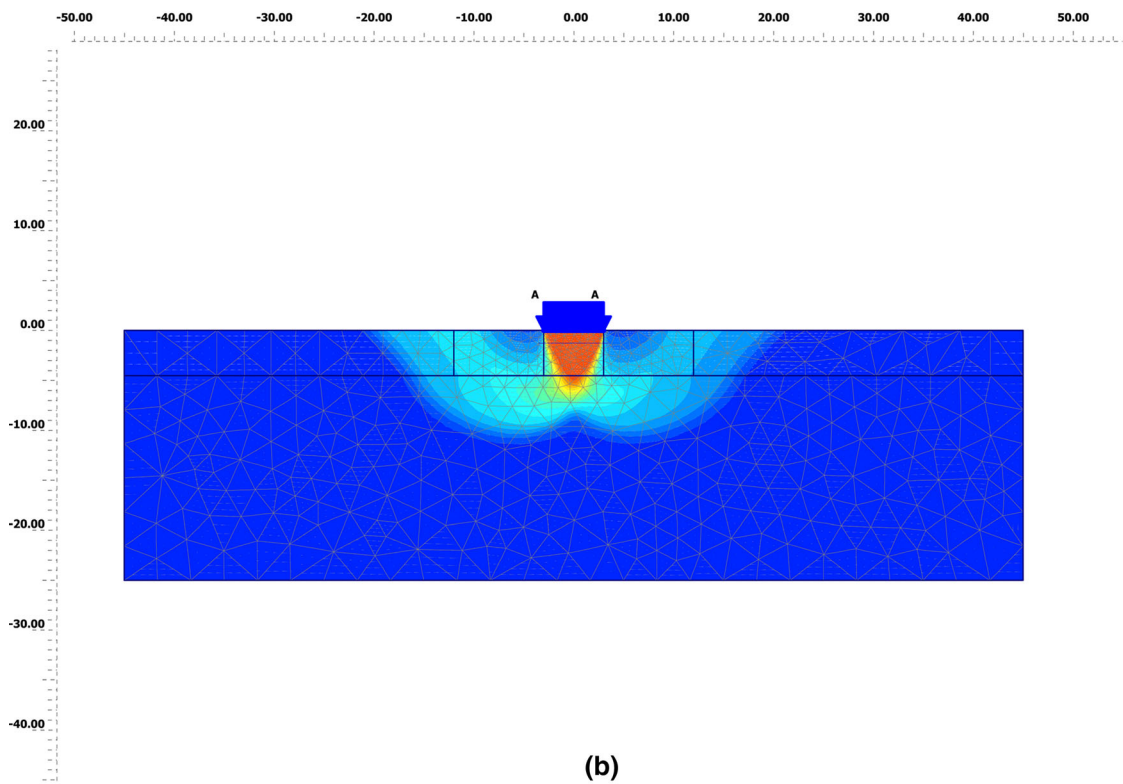
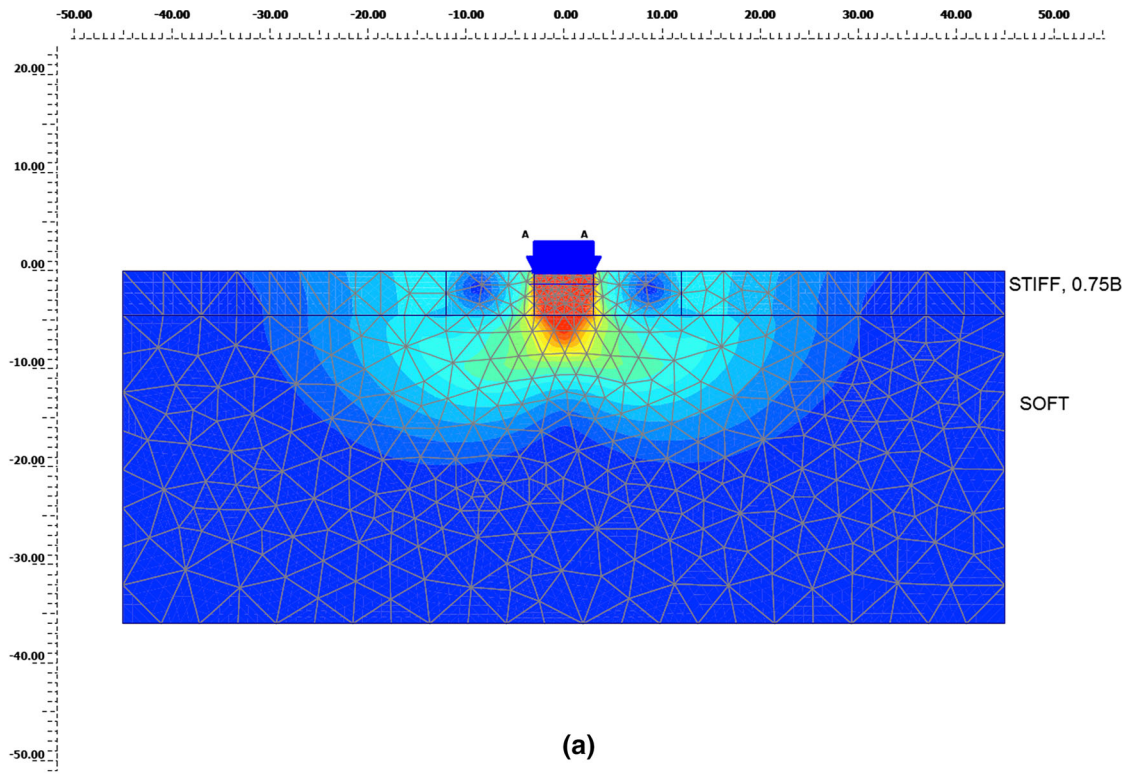


**Fig. 5** Strip footing on two-clay stratum, for  $H_1/B = 0.75$ : **a**  $SR = 0.133$ , **b**  $SR = 0.40$ , **c**  $SR = 0.80$

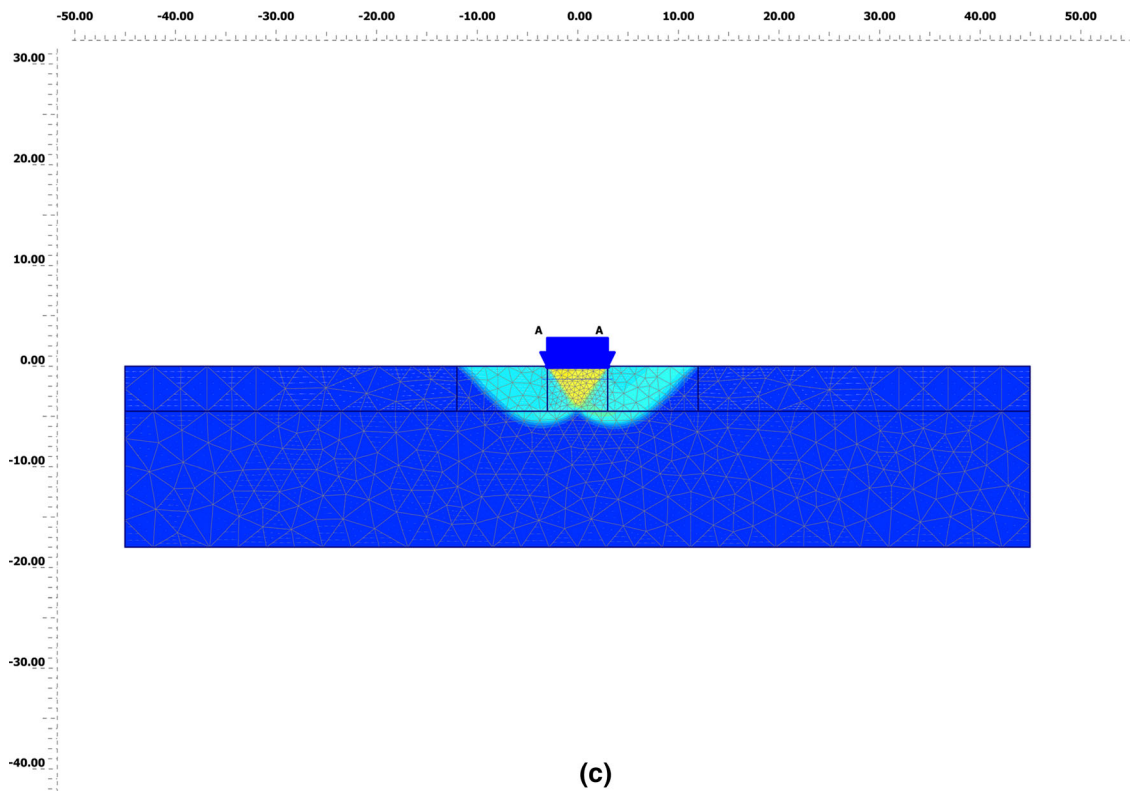
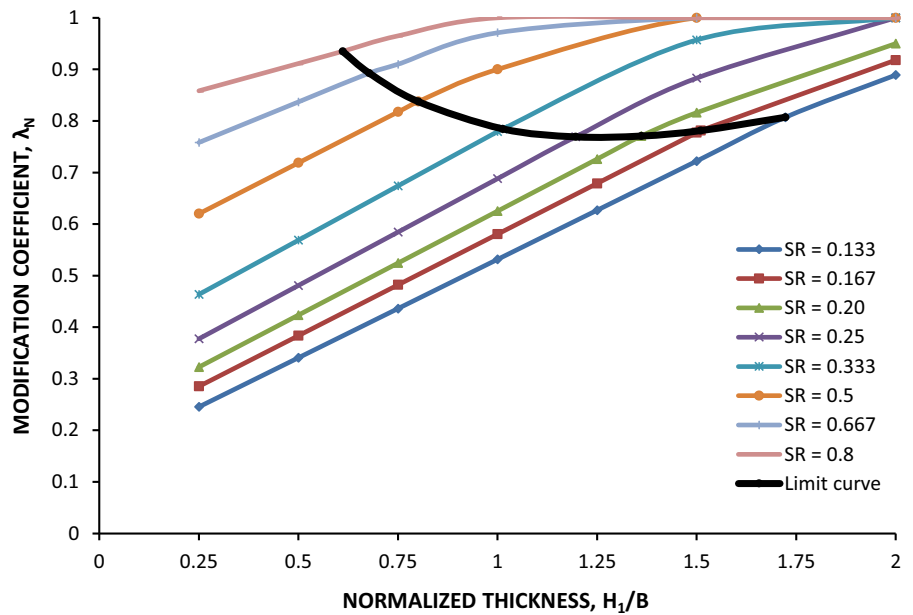


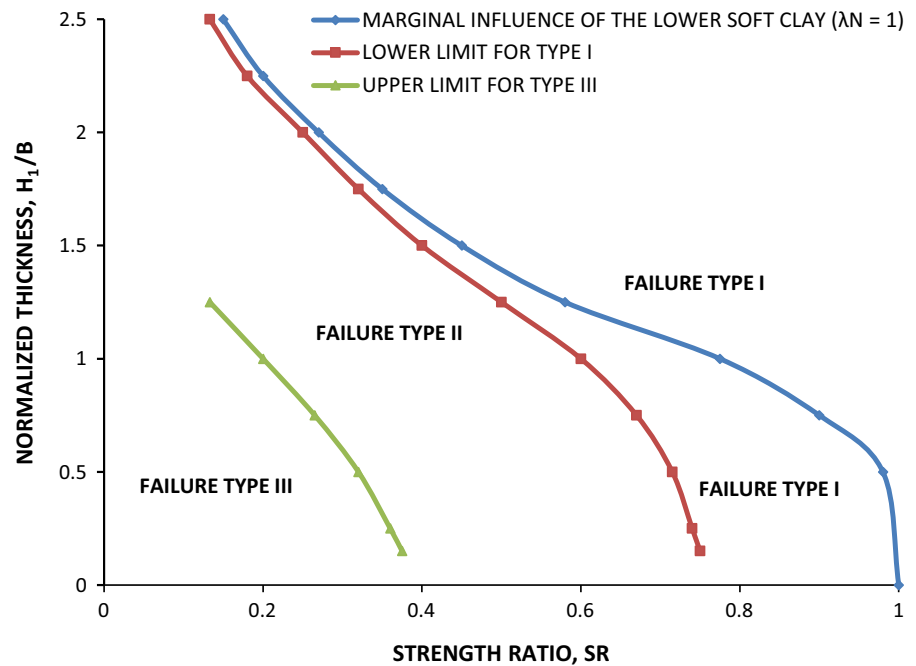
Fig. 5 continued

Fig. 6 Strip footing: Marginal combinations of  $H_1/B$  – SR for linear relationship between  $\lambda_N$  and  $H_1/B$





**Fig. 7** Strip footing, failure types depending on the combinations  $H_1/B$ , SR



clay layers on the bearing capacity, in case of punching failure. The correction coefficients  $\lambda_H$  and  $\lambda_B$  are given by the following algebraic expressions, best fitted the analyses results.

$$\lambda_H = [0.810 + 1.708(SR) - 2.518(SR)^2] \tag{9a}$$

and

$$\lambda_B = [1 + 0.17(1-SR)^2] \tag{9b}$$

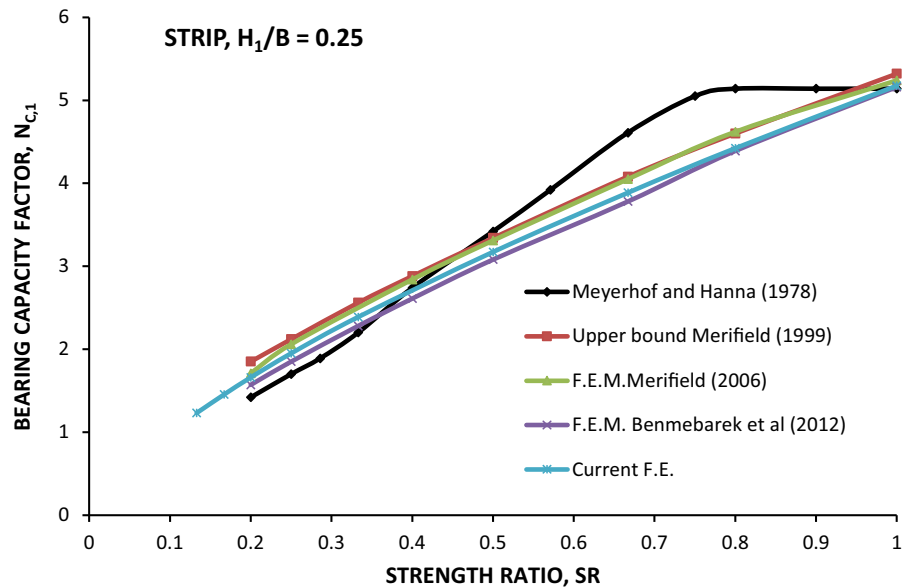
Note that the correction factor  $\lambda_H$  is almost equal to 1 for  $SR \leq 0.6$ , but it rapidly drops for higher values of the strength ratio. In contrast, the factor  $\lambda_B$  is always slightly higher of 1. For the special case of homogeneous soil ( $s_{u,2} = s_{u,1}$ ), it is obvious that  $\lambda_H = 0$  and  $\lambda_B = 1$ , since the Prandtl’s failure mechanism is developed. The limit curve illustrating the marginal correlation between  $H_1/B$ , SR and  $\lambda_N$ , for which Eqs. (8b), (9a) and (9b) are valid (punching or even partial failure) is also presented in Fig. 6. This marginal relationship between  $H_1/B$  and SR can be calculated by the following expression, valid for  $SR < 0.8$ :

$$(H_1/B) = 0.537(SR)^{-0.578} \tag{10}$$

The lower bound of  $H_1/B$  and SR, for which  $\lambda_N = 1$ , is presented in Fig. 7. Just below the curve,

the weaker clay marginally influences the bearing capacity. Evidently, for higher values the modification coefficient  $\lambda_N$  is equal to 1, while below the curve  $\lambda_N < 1$ , generally. In Fig. 7 the combinations of  $H_1/B$  and SR are also presented for failure type I (lower bound) and type III (upper bound). The intermediate zone corresponds to failure type II. It can be shown that failure type I is possible for  $SR > 0.75$ , independently of normalized thickness. It is also obvious from Fig. 7, that punching failure (III) is possible only for  $SR < 0.4$  and  $H_1/B < 1.25$  in the range of strength ratio investigated ( $SR \geq 0.133$ ). Merifield and Nguyen (2006) suggested that full punching shear failure develops for low strength ratios  $SR < 0.33$  and if  $H_1/B \leq 0.75$ , while general shear failure is possible for  $H_1/B \geq 1$ , in all SR cases. These trends seem similar with those of Fig. 7, although in the present paper more detailed results are illustrated. From the comparative presentation of the factor  $N_{C,1}$  in Fig. 8, it is evident that the current F.E. analyses are in good agreement with most of the previously proposed, slightly higher than Benmebarek’s et al. (2012) and lower than the upper bound of Merifield et al. (1999). The results after Meyerhof and Hanna (1978) deviate somewhat for  $SR \geq 0.6$ .

**Fig. 8** Comparison of  $N_{C,1}$  values for centrally loaded strip footing (Case  $SR < 1$ )



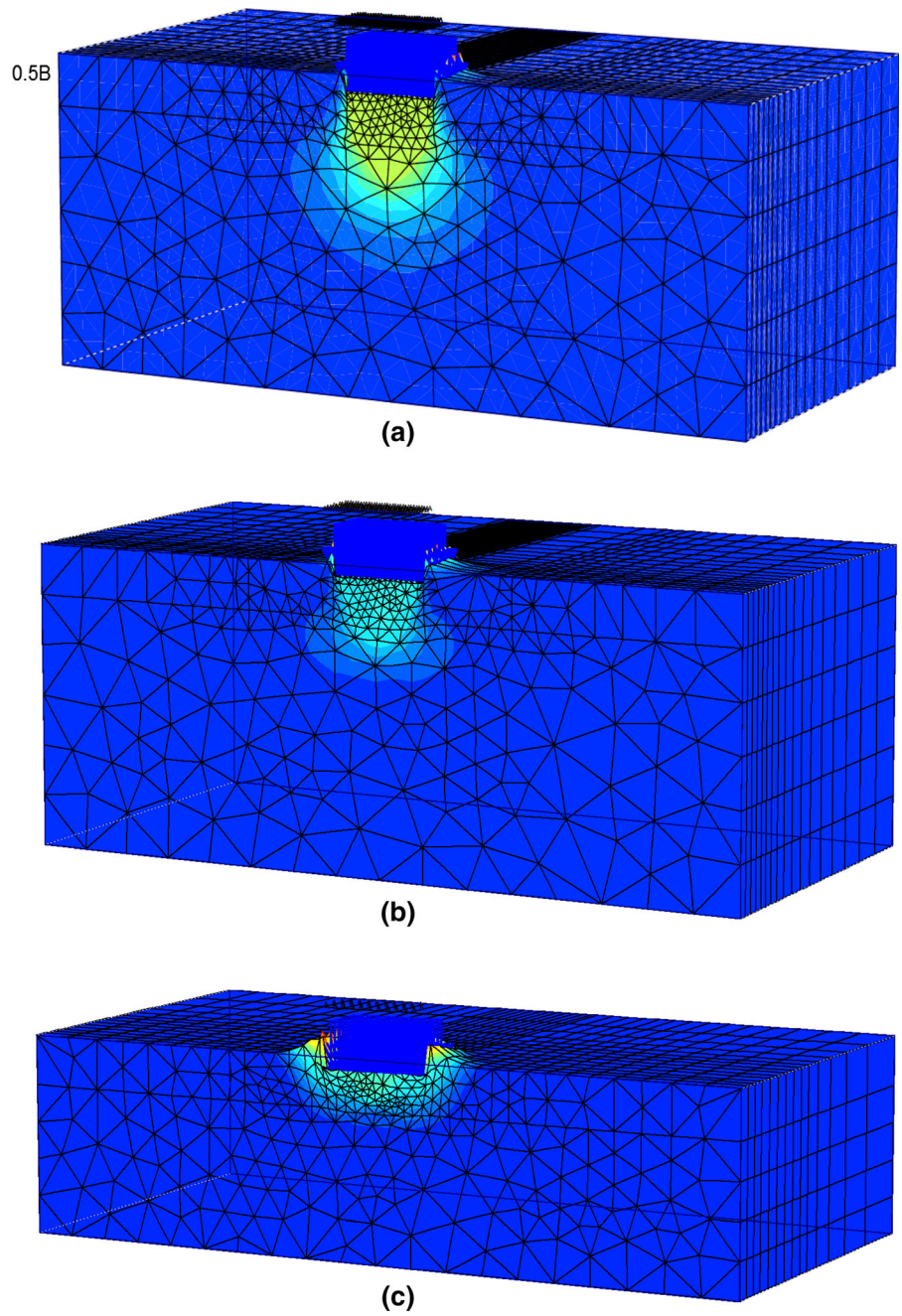
#### 4.2 Square and Rectangular Footings

The failure mechanisms are similar to those for strips (types I, II, III). However, the comparison of failure surfaces for strips or square footings is only qualitative, since in 3D conditions only the cross-section of these surfaces by the vertical plane of symmetry is conveniently presented and interpreted. Figure 9 illustrates these three mechanisms for a square footing in two clay layers with  $H_1/B = 0.50$ . Case (a) refers to low strength ratio  $SR = 0.133$ , where a punching failure develops, while a partial punching is shown in case (b) with  $SR = 0.40$ . For  $SR = 0.80$ , case (c), the mechanism approaches Prandtl's, type I. For square footings, the results of 3D F.E. analyses are summarized in Fig. 10, in which the bearing capacity factor  $N_{C,1}^*$  is plotted versus the strength ratio for six values of the normalized crust thickness. Note that  $N_{C,1}^*$  values quickly approach the  $N_C^*$  values of the homogeneous half space, for  $H_1/B \geq 0.50$  and  $SR \geq 0.50$ . From the comparative diagrams of Fig. 11, it is shown that our results for square footings approach well those of Merifield and Nguyen (2006), being about 1–5% higher. Note that the influence of the in situ stress field was not taken into account by Merifield and Nguyen

(2006). As already mentioned, for  $SR < 1$ , of weightless upper layer might result into slightly lower values of bearing capacity.

To further visualize the effect of the lower weaker clay layer, the modification coefficients ( $\lambda_N = N_{C,1}/N_C$  and  $\lambda_N^* = N_{C,1}^*/N_C^*$ ) are presented in Fig. 12 for strip and square footings respectively. Furthermore, for three cases of  $H_1/B$  presented in Fig. 12, it is clear that  $\lambda_N^* > \lambda_N$ , that is for a square foundation the unfavourable effect of lower clay is smaller than for a strip. It can be also observed that with increasing normalized thickness of the upper layer, the contrast between square and strip, expressed with the ratio  $\lambda_N^*/\lambda_N (> 1)$  also increases, reaching the value of 1.70 for low strength ratios and  $H_1/B = 0.75$ . From a practical point of view, for a square footing and normalized thickness  $H_1/B \geq 0.50$ , it is concluded that the lower weaker clay layer may be ignored, if  $SR \geq 2/3$ . On the contrary, for strip footings, the effects of the second layer are more significant, while even in case of  $H_1/B \geq 0.75$ , the weaker lower layer must be taken into consideration, regardless of a relatively high strength ratio. Comparison of the modification coefficient for strip  $\lambda_N$ , with  $\lambda_N^*$  for three cases of rectangular footings, is presented in Table 2.

**Fig. 9** Square footing on two-clay layers, for  $H_1/B = 0.50$ : **a**  $SR = 0.133$ , **b**  $SR = 0.40$ , **c**  $SR = 0.80$



The influence of shape of a rectangular ( $B, L$ ) footing on the bearing capacity can be also investigated through the shape factor  $s_c = N_{C,1}^*/N_{C,1}$ . The

variation of  $s_c$  with strength ratio  $SR$  is plotted in Fig. 13 for two values of  $H_1/B$  and three aspect ratios of rectangular footings ( $L/B = 1, 1.5, 3.0$ ). Evidently,

**Fig. 10** Square footing: Effect of  $H_1/B$  and SR on the factor  $N_{C,1}^*$

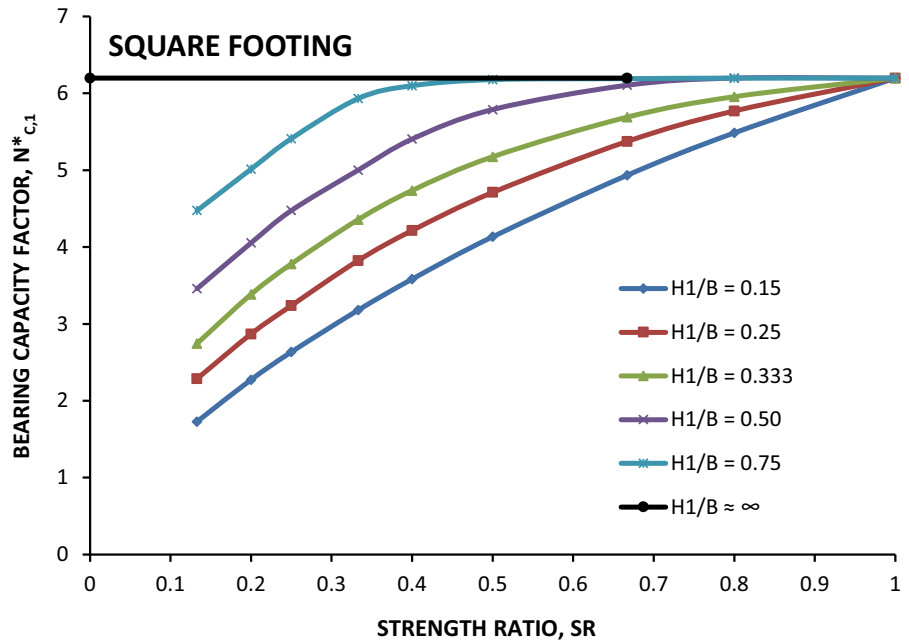
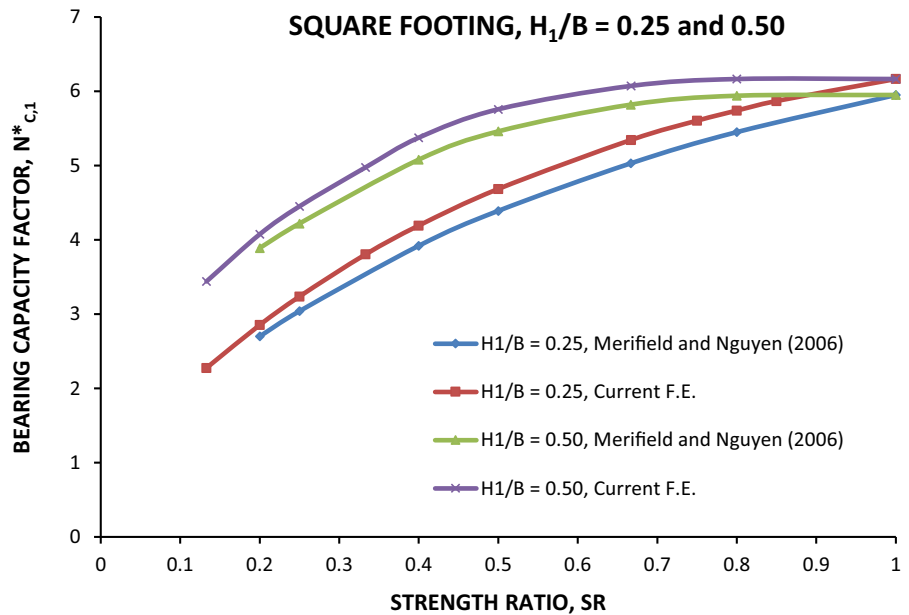


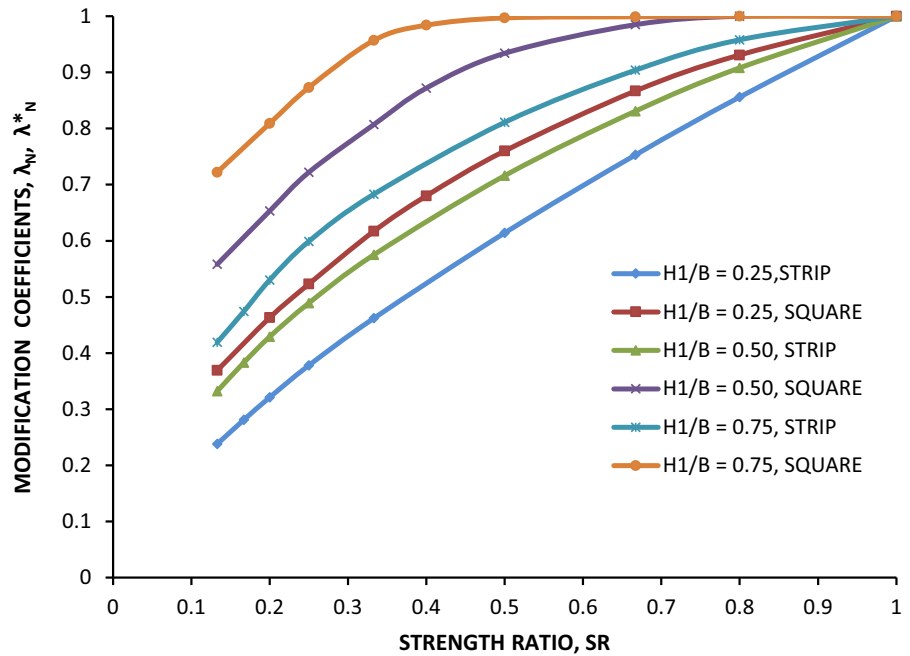
**Fig. 11** Comparison of  $N_{C,1}$  values for centrally loaded square footing (Case  $SR < 1$ )



for  $L/B = \infty$ ,  $s_c = 1$  in any case. Invariably, the shape factor increases when the ratio SR decreases, with the square factor tending to 1.2 as SR tends to 1 (homogeneous soil). Evidently, for strip foundations, the influence of the lower weaker layer is more

important. On the contrary, when the aspect ratio  $L/B$  decreases, the strength of the upper layer has the dominant effect on the bearing capacity. Note that for  $H_1/B = 0.50$  the shape factor for square footing and the lowest examined ratio  $SR = 0.133$  (i.e.  $s_{u,1} = 7.5$

**Fig. 12** Comparison of modification coefficients for strip and square rigid footings ( $SR < 1$ )



$s_{u,2}$ ) is  $s_c \approx 2.0$ , while for homogeneous soil  $s_c \approx 1.2$ .

4.3 Ring Footings

For ring foundations, the analyses are carried out under axisymmetric conditions, where the central axis of the ring is set at the left vertical boundary of the mesh. Now, three parameters influence the bearing capacity (Fig. 1b): the strength ratio  $SR$ , the

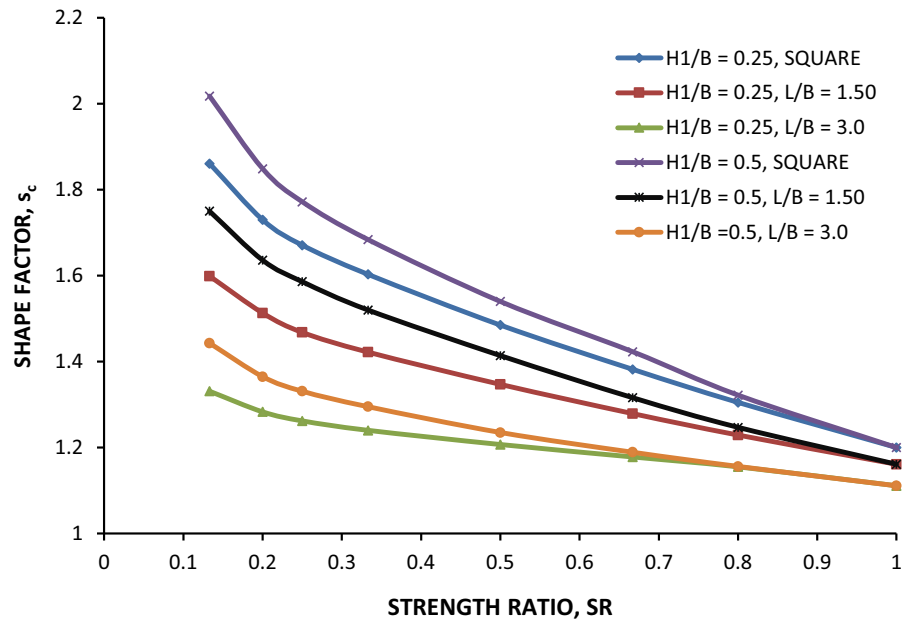
normalized thickness of the upper layer,  $H_1/2R_1 = H_1/B$  and the geometry of ring, which is defined by the normalized width,  $b/R_1$ . The three types of failure mechanism, slightly modified, are developed (depending on the above parameters). An example is given in Fig. 14 for constant  $H_1/B = 0.25$  (or  $H_1/R_1 = 0.50$ ),  $SR = 0.25$  and varying normalized width of the ring. For the higher value  $b/R_1 = 0.75$  (case a), punching type failure is observed, while for the lower  $b/R_1 = 0.25$  (case c), the failure mode in the radial

**Table 2** Modification coefficients  $\lambda_N, \lambda_N^*$  for rectangular footings

SR	$H_1/B = 0.25$				$H_1/B = 0.50$				$H_1/B = 0.75$			
	Strip	L/B = 3	L/B = 1.5	Square	Strip	L/B = 3	L/B = 1.5	Square	Strip	L/B = 3	L/B = 1.5	Square
0.133	0.238	0.285	0.328	0.369	0.332	0.432	0.5	0.558	0.419	0.573	0.645	0.722
0.2	0.321	0.370	0.418	0.463	0.429	0.527	0.605	0.653	0.53	0.680	0.745	0.809
0.25	0.378	0.429	0.478	0.523	0.489	0.586	0.668	0.722	0.599	0.741	0.809	0.873
0.333	0.462	0.516	0.566	0.617	0.575	0.67	0.753	0.807	0.683	0.817	0.894	0.957
0.5	0.614	0.667	0.712	0.76	0.716	0.796	0.872	0.934	0.811	0.914	0.983	0.997
0.667	0.753	0.798	0.83	0.867	0.831	0.889	0.942	0.985	0.904	0.970	0.998	0.999
0.8	0.856	0.89	0.906	0.931	0.908	0.945	0.975	1	0.958	0.993	1	1
1	1	1	1	1	1	1	1	1	1	1	1	1



**Fig. 13** Shape factor  $s_c$  for rectangular footings, as function of the strength ratio



plane is similar to Prandtl's (type I), although it is almost imperceptibly asymmetric. Evidently, as  $b/R_1$  tends to 0, the failure mechanism on the radial plane is almost the same with a strip footing (Prandtl's mechanism). At the other extreme, as  $b/R_1$  increases approaching 1, the footing approaches the circle and the failure mechanism is of scoop type encompassing the whole foundation (similar to Fig. 14a). The B.C. factor  $N_{C,1}^*$  is given in Fig. 15 for two values of  $H_1/R_1$ , 0.25 and 0.5 and five values of  $b/R_1$ . For low SR values,  $N_{C,1}^*$  increases with decreasing  $b/R_1$ . On the contrary, for high strength ratios (i.e.  $SR \geq 0.80$ ), the higher values of  $N_{C,1}^*$  correspond to circle. Comparison of the modification coefficients  $\lambda_N^*$  for five values of  $b/R_1$  is presented in Table 3. Obviously, the shape effects of a ring foundation can be considered by two ways: (a) For constant  $H_1/R_1$  (i.e. constant  $H_1/B$ , where the diameter  $B = 2R_1$ ) and varying normalized width  $b/R_1$ . (b) For constant  $H_1/b$  and varying radius  $R_1$  (or varying  $H_1/B$ ). The shape factor is calculated, as  $s_c = N_{C,1}^*/N_{C,1}$ , where  $N_{C,1}$  corresponds to strip ( $B = 2R_1$ ). It is evident that for decreasing  $b/R_1$ , the factor  $s_c = N_{C,1}^*/N_{C,1}$  increases, as illustrated in Fig. 16, where for low  $SR = 0.133$  reaches values as

high as 3. In case of constant  $H_1/b$ , both the varying ratios  $H_1/R$  and  $b/R_1$  affect the bearing capacity. Now the higher values of  $s_c$  correspond to full circle, as indicated in Fig. 17, while for low values  $b/R_1$ , the behaviour of the ring approaches this of a strip.

## 5 Soft Over Stiff Clay Layer

### 5.1 Strip Footing

Two basic types of failure are ascertained in our parametric analyses:

- The failure surface is extended into the lower, stiff or very stiff clay layer (type IV). This kind of failure is observed for low values of the normalized thickness  $H_1/B$  and/or for strength ratios only slightly higher than the unity.
- The failure surface is restricted into the top layer only (type V) for either high values of  $H_1/B$  or high values of SR.

Figure 18 illustrates these two mechanisms for  $H_1/B = 0.25$  and strength ratios (a)  $SR = 1.25$  and (b)  $SR = 2.5$ . In case (a), the failure mode is similar

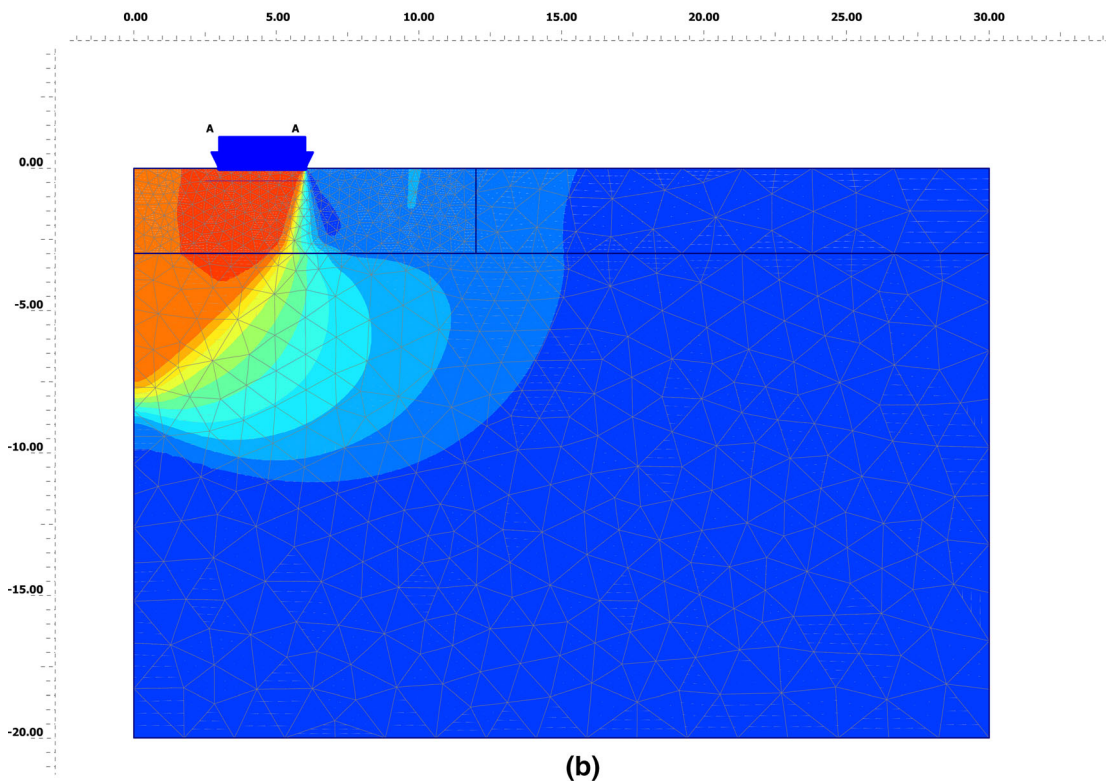
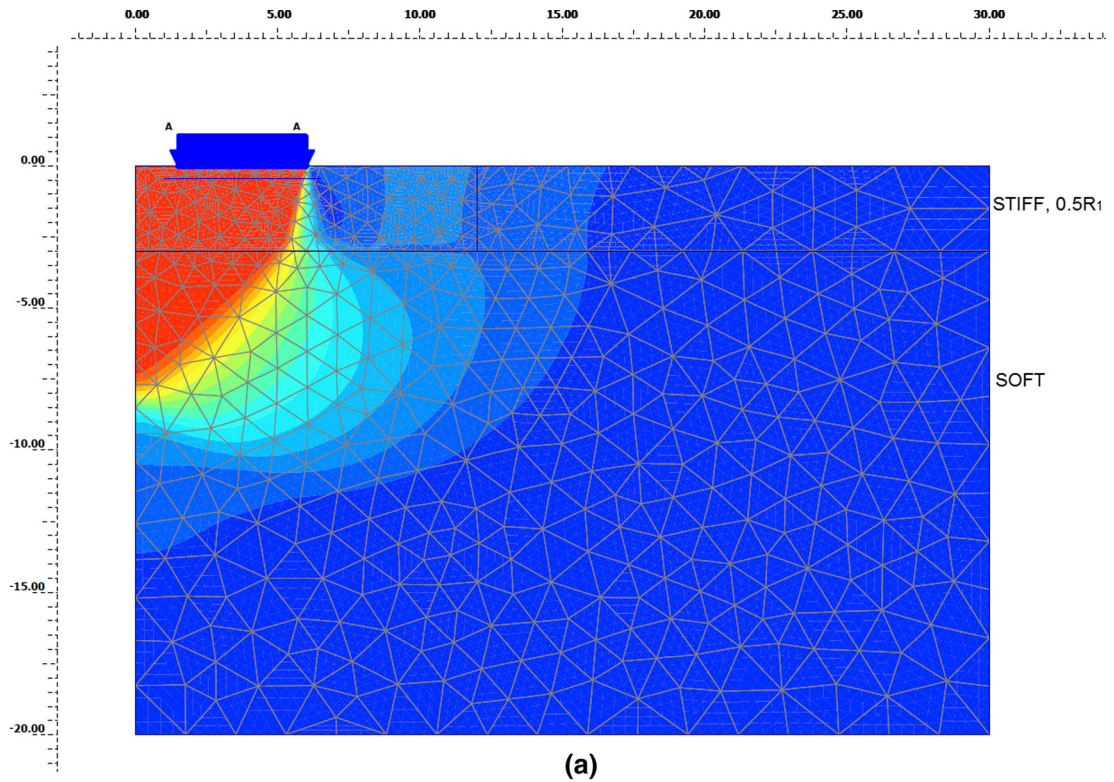


**Fig. 14** Deformation pattern at failure for ring footings:  $H_1/R_1 = 0.50$  and  $SR = 0.25$ : **a**  $b/R_1 = 0.75$ , **b**  $b/R_1 = 0.50$ , **c**  $b/R_1 = 0.25$

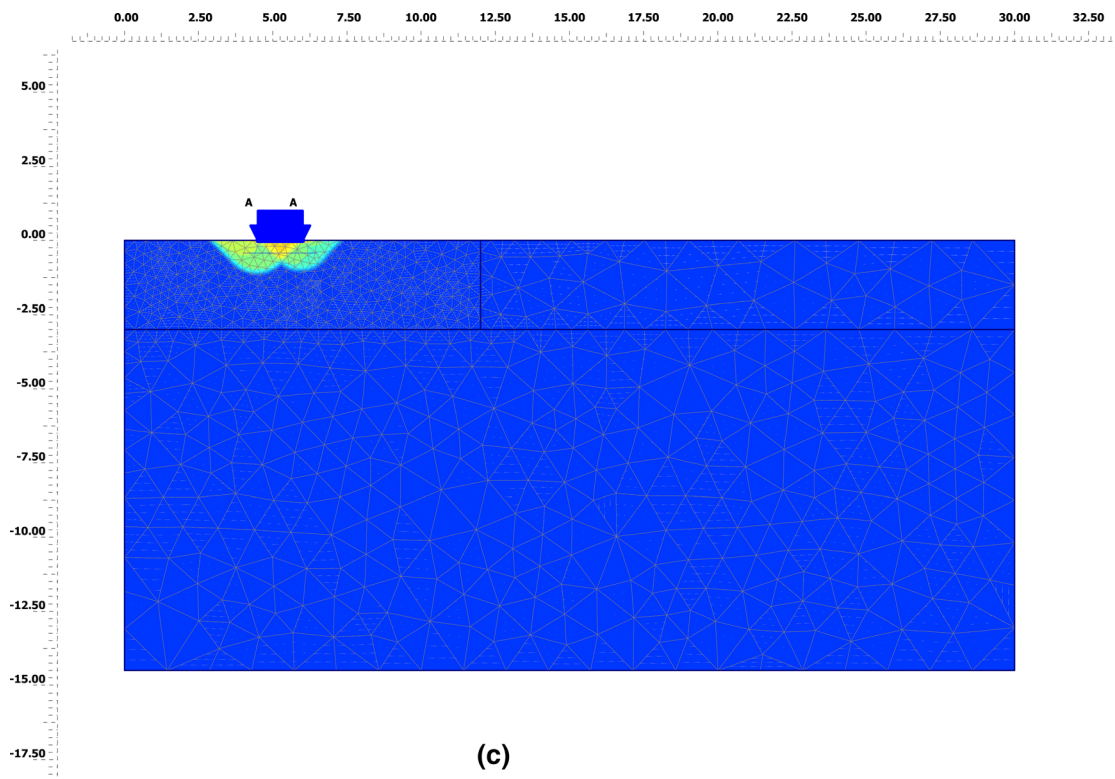


Fig. 14 continued

to Prandtl's, but secondary surfaces are observed at the edges of the strip, into the upper weaker clay layer (type IV). In case (b), the failure is clearly restricted to the upper layer (type V). The variation of the bearing capacity factor  $N_{C,1}$ , according to Eq. (2), is presented in Fig. 19, as function of the strength ratio SR for three representative values of the normalized thickness,  $H_1/B$ . Therefore, the following conclusions may be drawn:

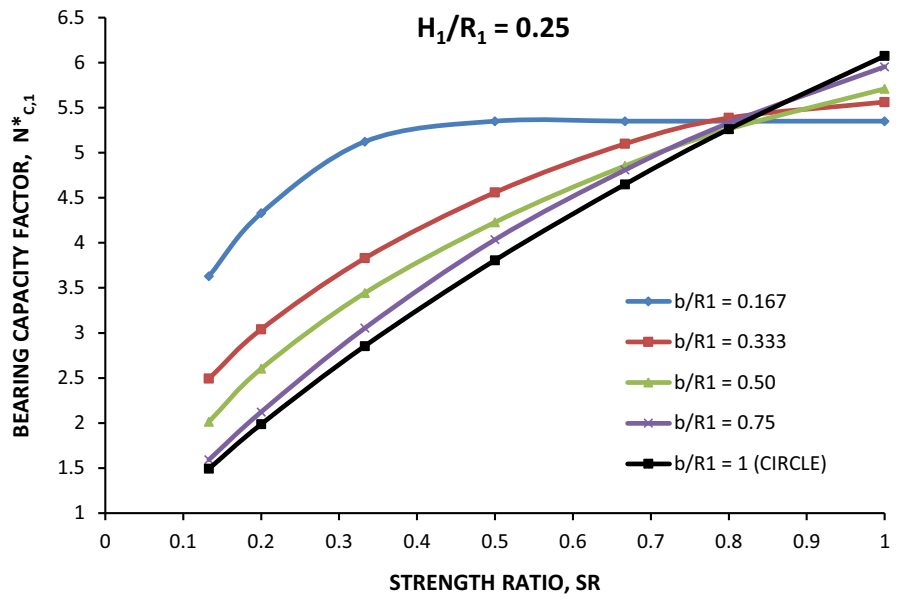
1. The factor  $N_{C,1}$  rapidly increases with increasing strength ratio, for SR slightly higher than the unity, reaching its maximum value for a critical value ( $SR_{cr}$ ), no particularly high. The failure type IV is observed for  $1 \leq SR \leq SR_{cr}$ . Evidently, the B.C. factor is stabilized to its  $\max N_{C,1}$  value for higher values than the critical, since the failure mechanism is restricted into the upper layer (type V).

2. For lower values of normalized thickness, higher values of the B.C. factor  $\max N_{C,1}$  are observed. Consequently, the maximum value of modification coefficient  $\lambda_N = N_{C,1}/N_C$  decreases with increasing  $H_1/B$ . For example, for  $H_1/B = 0.4$  (Fig. 19)  $\max \lambda_N \approx 1.07$  (relatively low). It may be concluded from the analyses that the favourable effect of the lower strong clay layer can be ignored for  $H_1/B \geq 0.5$  independently of the strength ratio. The maximum values of the modification coefficient,  $\max \lambda_N$  can be calculated by a closed form equation for strip, best fitting the F.E. results:

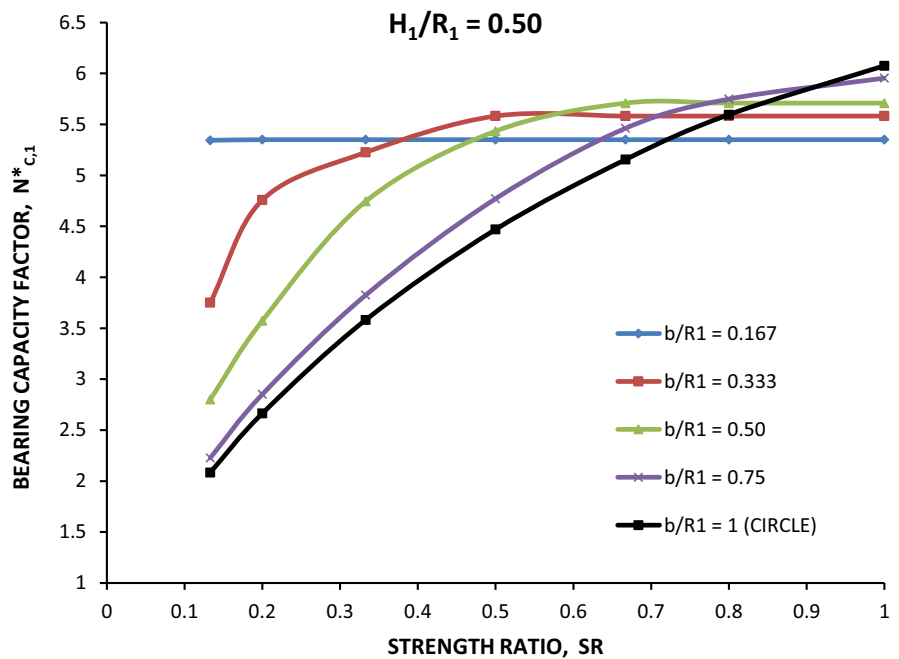
$$\max \lambda_N = \max N_{C,1}/N_C = 0.092 \frac{B}{H_1} + 0.869 \quad (11)$$

This equation is valid for  $H_1/B < 0.7$ , since for  $H_1/B \geq 0.7$ ,  $\max N_{C,1} = N_C \approx 5.164$ , so the lower clay

**Fig. 15** Effect of the normalized width and SR on the B.C. factor for ring foundations ( $SR < 1$ )



(a)



(b)

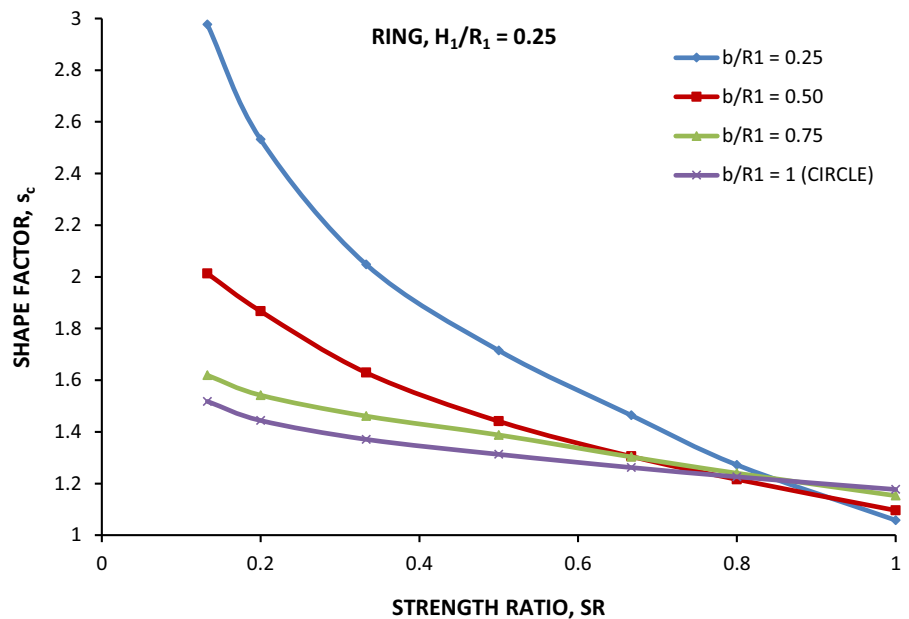
has no effect on the bearing capacity, regardless of the strength ratio  $SR$ . The critical strength ratio,  $(SR)_{cr}$ , for given values of the normalized thickness,  $H_1/B$ , is of

peculiar interest. From regression analysis of the F.E. analyses the following relationship results, which is also valid for  $H_1/B < 0.7$ :

**Table 3** Modification coefficient  $\lambda_{N_c}^*$  for ring footings

SR	$H_1/R_1 = 0.25$					$H_1/R_1 = 0.50$				
	$b/R_1 = 0.167$	$b/R_1 = 0.333$	$b/R_1 = 0.5$	$b/R_1 = 0.75$	$b/R_1 = 1$	$b/R_1 = 0.167$	$b/R_1 = 0.333$	$b/R_1 = 0.5$	$b/R_1 = 0.75$	$b/R_1 = 1$
0.133	0.679	0.448	0.353	0.268	0.246	0.998	0.672	0.490	0.374	0.343
0.2	0.809	0.547	0.456	0.357	0.327	1	0.852	0.626	0.479	0.438
0.333	0.958	0.688	0.603	0.513	0.470	1	0.936	0.831	0.642	0.590
0.5	1	0.820	0.741	0.678	0.627	1	1	0.952	0.801	0.736
0.667	1	0.917	0.850	0.808	0.766	1	1	1	0.917	0.848
0.8	1	0.968	0.922	0.895	0.866	1	1	1	0.966	0.921
1	1	1	1	1	1	1	1	1	1	1

**Fig. 16** Shape factors for ring with constant  $H_1/R_1 = 0.25$  and varying width  $b$



$$(SR)_{cr} = 0.176 \frac{B}{H_1} + 0.752 \tag{12}$$

5.2 Square Footings

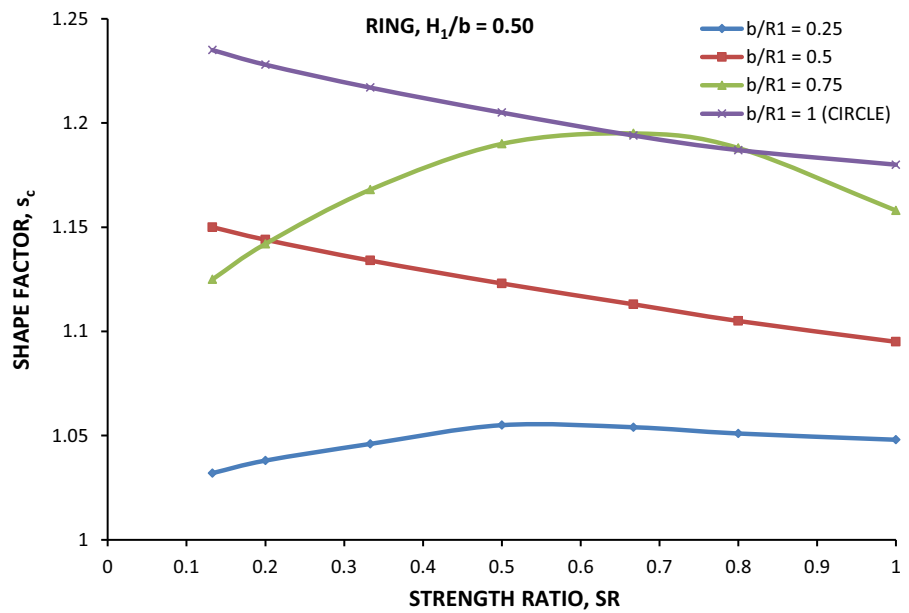
The failure mechanisms in the special case of square footings, are similar to those for strips (types IV and V). For either high values of  $H_1/B$  and/or high SR, the failure surfaces are developed in the upper layer, otherwise they extended into the second, stronger one. However, a direct comparison of the failure mechanism either in plane strain (strip) or in 3D conditions

(square) is only qualitative. In the latter case, the only one representative cross-section of the failure surface by the central vertical plane is considered.

The bearing capacity factor  $N_{C,1}^*$ , according to Eq. (4) from the 3D F.E. analyses, is presented in Fig. 20 versus SR for various values of  $H_1/B$ . The trends are similar with those observed in Fig. 19 for strip footings. Interestingly, for  $H_1/B \geq 0.50$ ,  $\max N_{C,1}^* = N_C^* \approx 6.2$ , thus the underlying stronger clay layer has no favourable effect on the bearing capacity. In any case, the increase of B.C. due to the second layer, in comparison with the homogeneous clays, is an interesting issue, which is investigated through the



**Fig. 17** Shape factors for ring with constant  $H_1/b$  and varying radius  $R_1$



corresponding modification coefficient  $\max \lambda_N^* = \max N_{C,1}^*/N_C^*$ . Performing the regression analysis, the following formula is resulted:

$$\max \lambda_N^* = 0.0054(B/H_1)^2 - 0.0049(B/H_1) + 0.9882 \tag{13}$$

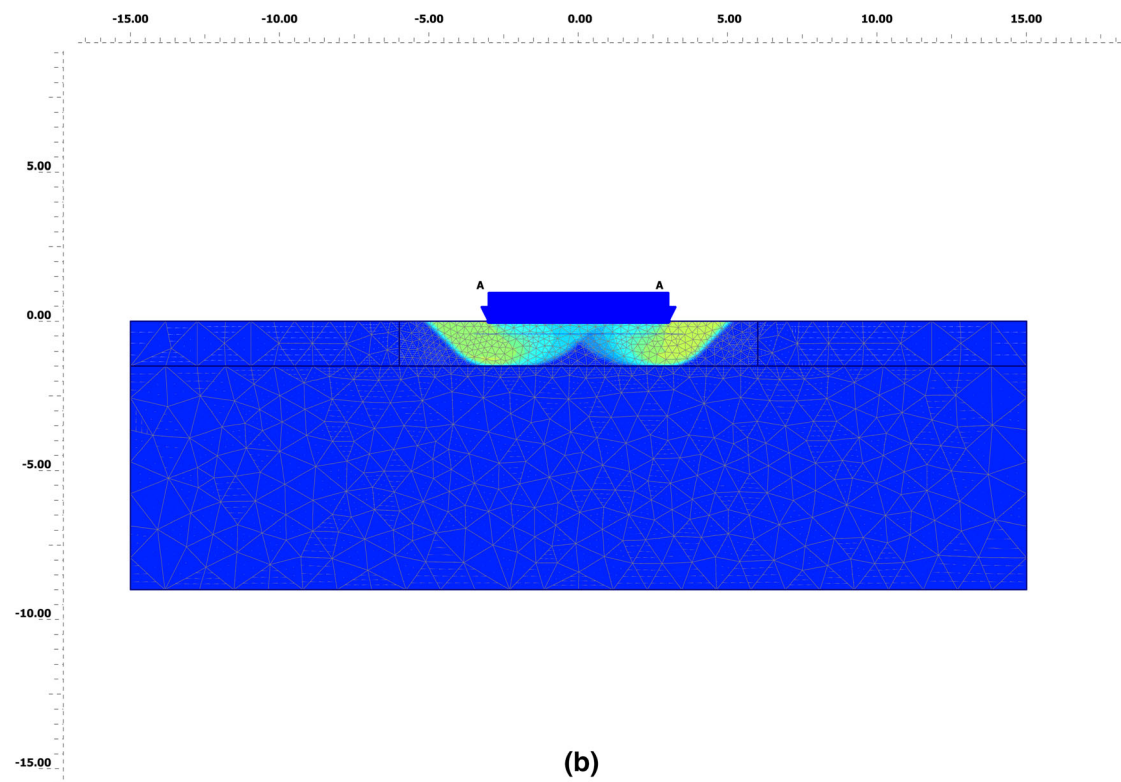
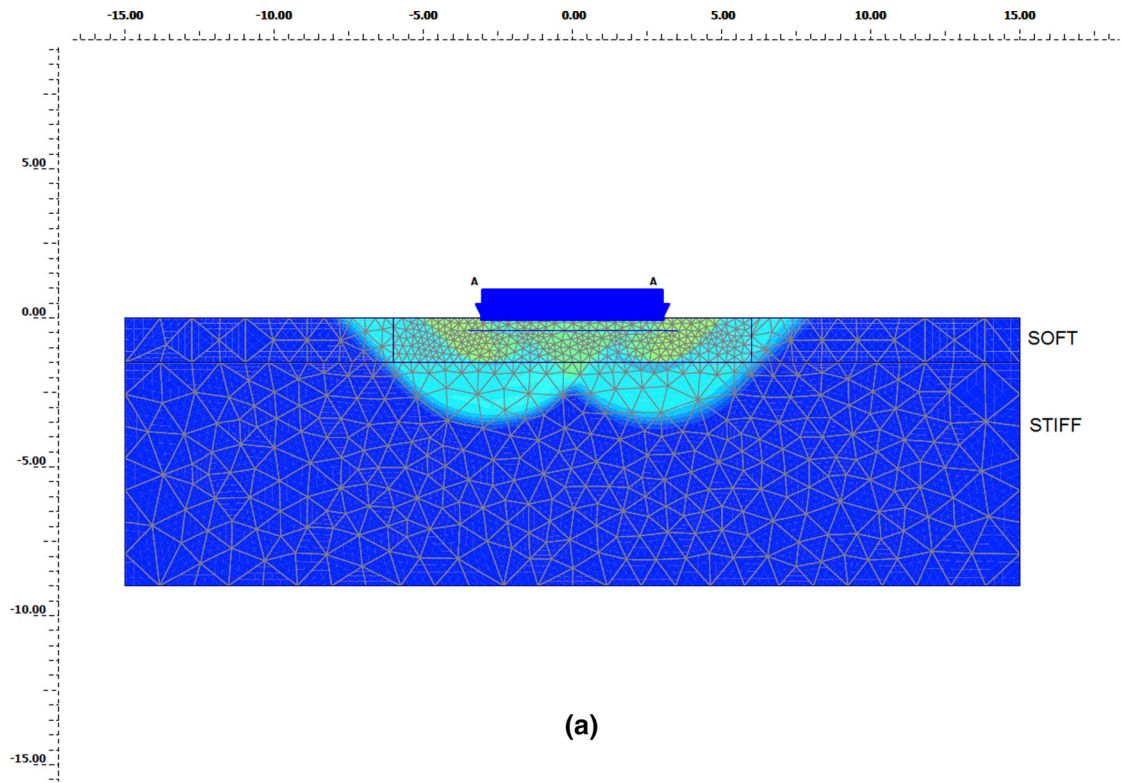
The equation is valid for  $H_1/B \leq 0.5$ , since for  $H_1/B \geq 0.5$ ,  $N_{C,1}^* = N_C^*$ . Figure 21 compares the maximum values of the modification coefficients  $\lambda_{N-} = N_{C,1}/N_C$  (strip) and  $\lambda_{N^*} = N_{C,1}^*/N_C^*$  (square and circle), which are plotted versus  $H_1/B$ . These values are of course independent of SR, as Figs. 19 and 20 show. We note that the strip footing «reaches deeper» than the square and hence more affected by  $H_1/B$ ; and that for  $H_1 > 0.5 B$ , the ultimate capacity of square is not influenced by SR.

### 5.3 Ring Footings

The B.C. factor  $N_{C,1}^*$  for the special case of a full circular footing ( $b/R_1 = 1$ ) is presented in Fig. 22 for various values of the strength ratio and the normalized thickness  $H_1/B$  (diameter,  $B = 2R_1$ ). It seems that for

$H_1/B \geq 0.25$  the lower clay layer has only a little impact on the bearing capacity, in this case with the circular footing. For example, if  $H_1/B \geq 0.40$ , the factor  $N_{C,1}^*$  is constant, irrespectively of the strength ratio. The maximum values of the modification coefficient,  $\max \lambda_N^*$  are already presented in Fig. 21 in comparison with the results for strip and square footings. It is clear that the favourable effects of the second hard layer on the B.C. are lower in the case of circle.

In the general case of ring footings, the failure mechanisms depend on both the ratios  $H_1/R_1$  and  $b_1/R_1$ , or alternatively on the normalized thickness  $H_1/b_1$  and  $b/R_1$ . For relatively low values of  $H_1/R_1$  and high  $b/R_1$ , a failure mechanism similar to type IV develops, while for higher values of  $H_1/R_1$  and/or lower  $b/R_1$ , the type V takes place. Figure 23 depicts the relationship between  $N_{C,1}^*$  and SR for various values  $b/R_1$ , in the case of low value  $H_1/R_1 = 0.15$ . The low values of  $b/R_1$  correspond to high values  $H_1/b$ , thus the lower, stronger clay layer has no influence on the bearing capacity and consequently it can be ignored. By contrast, for higher values  $b/R_1$ , the ratio  $H_1/b$  is low



◀ **Fig. 18** Deformation pattern at failure for strip footing on soft over stiff clay,  $H_1/B = 0.25$ : Failure mechanisms: **a**  $SR = 1.25$ , Type IV, **b**  $SR = 2.5$ , Type V

enough, and now the second layer has a significant effect on the bearing capacity. For the full circle ( $b/R_1 = 1$ ), the B.C. factor reaches the max  $N_{c,1}^*$  value for

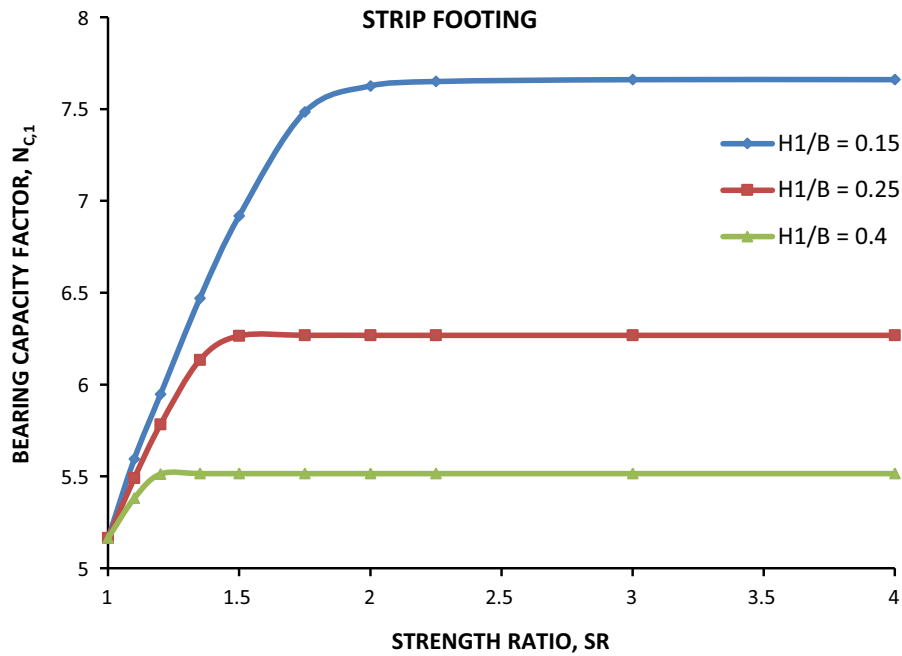


**Fig. 19** Effect of  $H_1/B$  and SR on the B.C. factor for strip footing on soft over stiff clay layer

**Fig. 20** B.C. factor for square footings as a function of  $H_1/B$  and SR

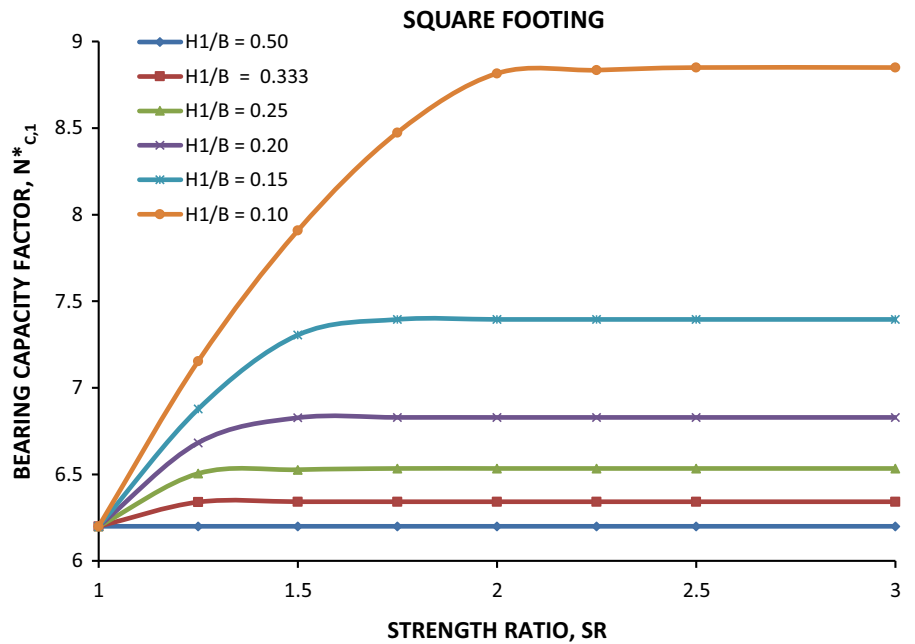


**Fig. 21** Soft over stiff clay layer: Comparison of maximum modification coefficients for strip, square and circle

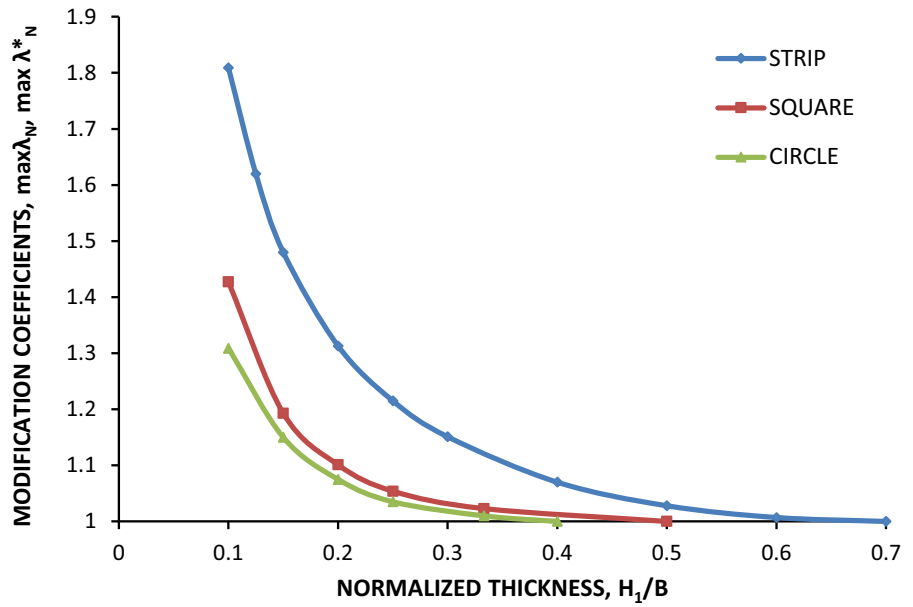
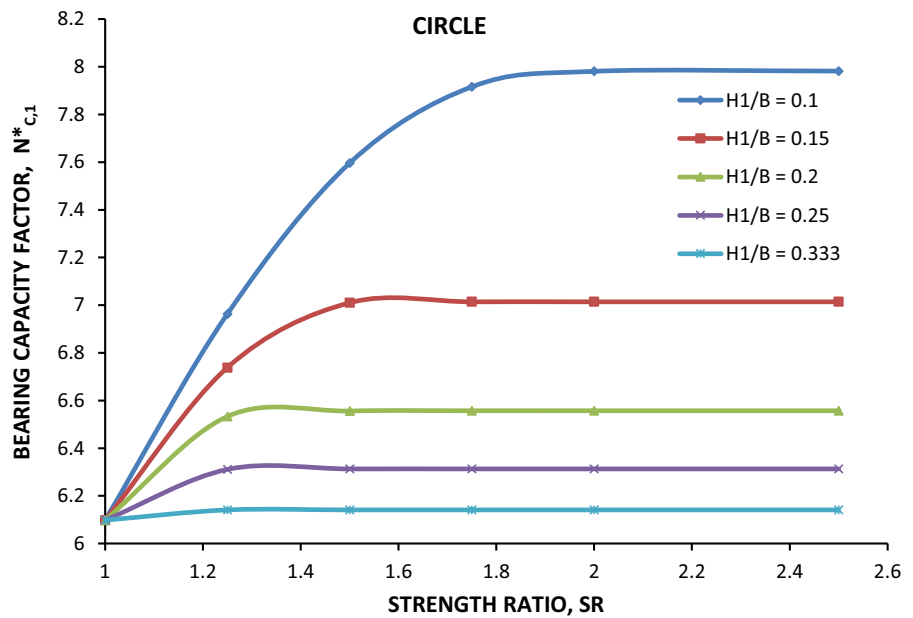


**Fig. 22** B.C. factor as function of the ratio SR for circle ( $B = 2R_1$ )

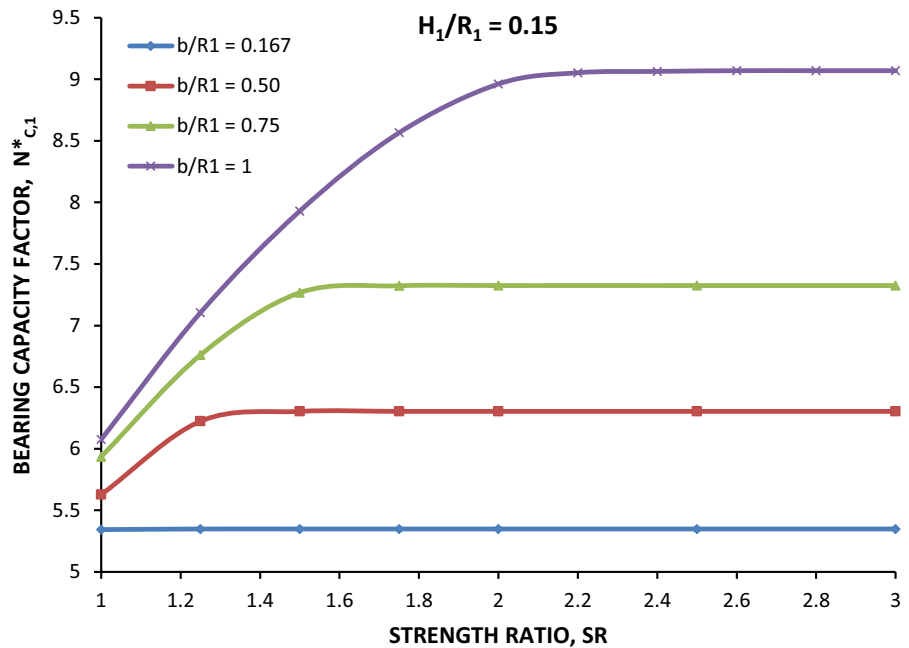


strength ratios  $SR \geq 2.40$  in this case of low  $H_1/B$ , the critical value  $(SR)_{cr}$  is quite lower for lower normalized widths  $(b/R_1)$  of a ring footing.

### 6 Conclusions

- (a) The F.E. results were firstly presented in terms of B.C. factors  $N_{C,1}$  or  $N_{C,1}^*$  (strip or other footing shape). The visual understanding of the

**Fig. 23** Effect of  $b/R_1$  and SR on the B.C. factor  $N_{C,1}^*$  for ring foundation



effects of second layer (either weaker or stronger) was facilitated by the modification coefficients  $\lambda_N$  or  $\lambda_N^*$ .

- (b) In the most interesting case of upper stiff crust ( $SR < 1$ ) and strip footings, three types of failure are ascertained. Bound values (combinations  $H_1/B$  and  $SR$ ) are presented for each of them (i.e. punching failure, type III seems possible if  $SR < 0.4$  and  $H_1/B < 1.25$ ). For a wide range of parameters, the B.C. factor  $N_{C,1}$  is linearly related with  $H_1/B$ . For rectangular or ring footings the failure mechanisms are modified accordingly. Modification coefficients  $\lambda_N$ ,  $\lambda_N^*$  and shape factors as well, are presented and discussed. In the case of ring footings,  $\lambda_N^*$  and  $s_c$  are strongly depended on  $b/R_1$  for given  $H_1/B$ .
- (c) For stiffer lower clay ( $SR > 1$ ) and strip footing, two additional types of failure are noted, while the modification coefficient ( $\lambda_N > 1$ ) rapidly increases with increasing  $SR$ , reaching the value  $\max \lambda_N$ . The bound values  $H_1/B$ , for which the favourable effect of the second layer becomes insignificant independently from  $SR$ , are estimated (i.e.  $H_1/B \geq 0.5$ ) or even lower for ring or square footings.
- (d) Closed form analytical expressions, best fitting the F.E. results, are proposed in several cases of

strip and square footings, either for  $SR < 1$  or  $SR > 1$ .

**References**

Benmebarek S, Benmoussa S, Belouar L, Benmebarek N (2012) Bearing capacity of shallow foundation on two clay layers by numerical approach. *J Geotech Geol Eng* 30:907–923

Brown JD, Meyerhof GG (1969) Experimental study on bearing capacity in layered clays. In: *Proceedings of 7th International Conference on Soil Mechanics and Foundation Engineering, Mexico*, vol 2, pp 45–51

Burd HJ, Frydman S (1997) Bearing capacity of plane strain footings on layered soils. *Can Geotech J* 34:241–253

Button SJ (1953) The bearing capacity of footings on a two-layer cohesive subsoil. In: *Proceedings of 3rd International Conference on Soil Mechanics and Foundation Engineering, Zurich*, vol 1, pp 332–335

Chen WF (1975) *Limit analysis and soil plasticity*. Elsevier, Amsterdam

Hansen JB (1970) A revised and extended formula for bearing capacity. *Bulletin* 28:5–11, Danish Geotechnical Institute

Lee JK, Jeony S, Lee S (2016) Undrained bearing capacity factors for ring footings in heterogeneous soil. *Comput Geotech* 75:103–111

Merifield RS, Nguyen VQ (2006) Two and three dimensional bearing capacity solutions for footings on two-layered clays. *Geomech Eng Int J* 1(2):151–162



- Merifield RS, Sloan SN, Yu HS (1999) Rigorous plasticity solutions for the bearing capacity of two-layered clays. *Géotechnique* 49(4):471–490
- Meyerhof GG, Hanna AM (1978) Ultimate bearing capacity of foundations on layered soils under inclined load. *Can Geotech J* 15:565–572
- Michalowski RL (2002) Collapse loads over two-layer clay foundation soils. *Soils Found* 42(1):1–7
- Michalowski RL, Shi L (1995) Bearing capacity of footings over two-layered foundation soils. *J Geotech Eng* 121:421–428
- Moayed RZ, Rashidian V, Izadi E (2012) Evaluation of bearing capacity of ring foundations on two-layered soil. *World Acad Sci Eng Technol* 6:950–954
- Nguyen VQ, Merifield RS (2012) Two and three dimensional undrained bearing capacity of embedded footings. *Aust Geomech* 47(2):25–40
- Poulos HG, Carter JP, Small JC (2001) Foundations and Retaining structures—research and practice. In: *General Report on Proceedings of 15th I.C.S.M.G.E.*, vol 4, pp 2527–2606
- Puzrin AM, Alonso E, Pinyol N (2010) *Geomechanics of failures*. Springer, New York
- Salgado R (2008) *The engineering of foundations*. McGraw-Hill, New York
- Salgado R, Lyamin AV, Sloan SW, Yu HS (2004) Two-and three-dimensional bearing capacity of foundations in clay. *Géotechnique* 54(5):297–306
- Salgado R, Lyamin A, Lim J (2013) Foundation failure case histories reexamined using modern geomechanics. In: *International conference on case histories in geotechnical engineering*, Paper No SOAP-9, Chicago
- Vesic AS (1975) Bearing capacity of shallow foundations. In: Winterkorn HF, Fang HY (eds) *Foundation engineering handbook*. Van Nostrand Reinhold, New York, pp 121–147
- Yu L, Liu J, Kong XJ, Hu Y (2011) Three-dimensional large deformation F.E. analysis of square footings in two-layered clays. *J Geotech Geoenviron Eng*, ASCE 137(1):52–58
- Zhu M (2004) Bearing capacity of strip footings on two-layer clay soil by finite element method. In: *Proceedings of Abaqus user's Conference*, pp 777–787
- Zhu M, Michalowski RL (2005) Bearing capacity of rectangular footings on two-layer clay. In: *Proceedings of 16th I.C.S.M.G.E.*, vol 2, pp 997–1000

**Publisher's Note** Springer Nature remains neutral with regard to jurisdictional claims in published maps and institutional affiliations.